NASA TM-87726

NASA-TM-87726 19860015192

NASA Technical Memorandum 87726

NONISENTROPIC UNSTEADY THREE DIMENSIONAL SMALL DISTURBANCE POTENTIAL THEORY

M. D. Gibbons

W. Whitlow, Jr.

M. H. Williams

APRIL 1986

National Aeronautics and Space Administration

Langley Research Center
Hampton, Virginia 23665

NONISENTROPIC UNSTEADY THREE DIMENSIONAL SMALL DISTURBANCE POTENTIAL THEORY

M. D. Gibbons
Purdue University
West Lafayette, IN 47907

W. Whitlow, Jr.
NASA Langley Research Center
Hampton, VA 23665-5225

M. H. Williams
Purdue University
West Lafayette, IN 47907

Abstract

Modifications that allow for more accurate modeling of flow fields when strong shocks are present have been made to three dimensional transonic small disturbance (TSD) potential theory. In addition, Engquist-Osher type-dependent differencing was incorporated into the solution algorithm. The modified theory was implemented and tested in the XTRAN3S computer code. Steady flows over a rectangular wing with a constant NACA 0012 airfoil section and an aspect ratio of 12 were calculated for freestream Mach numbers (M_∞) of 0.82, 0.84, and 0.86. Comparisons between results obtained using the modified and unmodified TSD theories are presented along with results from a three dimensional Euler code. Nonunique solutions in three dimensions are shown to appear for the rectangular wing as aspect ratio increases. Steady and unsteady results are shown for the RAE tailplane model at $M_\infty = 0.90$. Comparisons are made between calculations using unmodified theory, modified theory and between experimental data.

Nomenclature

a^*	critical speed of sound
A	M_∞^2
AR	wing aspect ratio
B	$2M_\infty^2$
b	semispan
C_L	wing lift coefficient
C_p	pressure coefficient
C_{ps}	entropy generated pressure coefficient
$\tilde{C}_p$	unsteady pressure coefficient first harmonic of C_p
c_r	reference chord
c_v	constant volume specific heat
E	$1 - M_\infty^2$
$f(x,t)$	instantaneous wing surface position
f_i i=0,1,2,3	flux terms in equations 1-5
F	$-1/2\ (\gamma+1)M_\infty^2$ (NASA Ames)
	$-1/2\ [3 - (2-\gamma)M_\infty^2]M_\infty^2$ (NLR)
G	$-1/2\ (\gamma-3)M_\infty^2$ (NASA Ames)
	$-1/2\ M_\infty^2$ (NLR)
H	$-\ (\gamma-1)M_\infty^2$ (NASA Ames)
	$-\ M_\infty^2$ (NLR)
k	reduced frequency ($\omega c_r/2U_\infty$)
M_∞	free stream Mach number
R	nondimensionalized critical speed of sound
t	nondimensionalized time in units of chords of travel
T	ratio of normal velocity downstream of shock to normal velocity upstream of shock
U_∞	free stream velocity
u	streamwise perturbation velocity
x,y,z	streamwise, spanwise, and vertical distance nondimensionalized by reference chord
α	angle of attack
γ	ratio of specific heats
Δ	jump in quantity
η	fraction of semispan
ϕ	small disturbance velocity potential
ω	angular frequency, $2\pi \cdot$Frequency

Subscripts

∞	free stream conditions
ℓ	section lift
L	lower surface
U	upper surface
tip	wing tip

Superscripts

*	sonic value

Introduction

When shock waves appear in flow fields, aerodynamic loads predicted using potential flow theory can be grossly inaccurate or even multivalued. The problem of nonuniqueness of full potential solutions was first discussed by Steinhoff and Jameson[1]. They found numerical evidence that it may be a property of the partial differential equation that describes the flow field. In two dimensions, potential flow theory can produce multiple (nonunique) steady state solutions for a fixed angle of attack and free stream Mach number. Three steady flows can exist, each satisfying the flow equations and the associated boundary conditions. This phenomenon occurs only when strong embedded shocks are present. Further research on the

nonuniqueness of full potential solutions was done by Salas and Gumbert[2] who demonstrated that the problem was not confined to a particular airfoil or flow condition. Later, Williams, Bland, and Edwards[3] showed that two dimensional transonic small disturbance theory also produces multiple solutions. This characteristic is a result of the assumptions of isentropic and irrotational flow made when reducing the Euler equations to the potential flow equations. There have been no reported cases of multiple solutions obtained when solving the Euler equations.

Because of the above problems, any structural analysis carried out using loads predicted using TSD theory cannot be considered reliable. The inaccuracy in the TSD theory is due to the way in which the computed shock waves are modeled. Classical TSD theory does not model the jump in entropy that a fluid particle experiences as it passes through a shock wave, and calculated shocks can have the wrong strength and the wrong location.

Fuglsang and Williams[4] addressed the problem of multiple solutions in 2-D TSD theory by making changes to the flow equations. They did this by modifying the streamwise flux (to improve the shock jump conditions), modeling the effects of the increased entropy by calculating the entropy jump through shocks and convecting it downstream, and corrected the pressure coefficient to take into account the effects of entropy. The modifications were implemented and tested in the XTRAN2L[5] code. The resulting method gave results that were in much better agreement with Euler solutions than calculations made with the unmodified TSD theory.

The purpose of this paper is to extend these nonisentropic modifications to three dimensional TSD theory. They have been implemented and tested in the XTRAN3S finite difference computer code[6]. The incorporation of these modifications into XTRAN3S, as will be shown, permits a more realistic modeling of transonic flow fields.

Governing Equations

The flow equation currently solved in XTRAN3S is

$$\frac{\partial f_0}{\partial t} + \frac{\partial f_1}{\partial x} + \frac{\partial f_2}{\partial y} + \frac{\partial f_3}{\partial z} = 0 \qquad (1)$$

where

$$f_0 = -(A\phi_t + B\phi_x) \qquad (2)$$

$$f_1 = E\phi_x + F\phi_x^2 + G\phi_y^2 \qquad (3)$$

$$f_2 = \phi_y + H\phi_x\phi_y \qquad (4)$$

$$f_3 = \phi_z \qquad (5)$$

The constants A, B, and E are defined as

$$A = M_\infty^2$$

$$B = 2M_\infty^2 \qquad (6)$$

$$E = 1 - M_\infty^2$$

The constants F, G, and H depend on the assumptions made in deriving the flow equation. In the current effort, two separate sets were used. The first set, known as the NASA/Ames coefficients[7], is

$$F = -1/2\ (\gamma+1)M_\infty^2$$

$$G = 1/2\ (\gamma-3)M_\infty^2 \qquad (7)$$

$$H = -\ (\gamma-1)M_\infty^2$$

These coefficients are obtained when the unsteady TSD equation is derived in a manner similar to the steady three dimensional equation developed by Lomax et al.[7]. The second set, or NLR coefficients,[8] are

$$F = -1/2[3 - (2-\gamma)M_\infty^2]M_\infty^2$$

$$G = -\ 1/2\ M_\infty^2 \qquad (8)$$

$$H = -\ M_\infty^2$$

These coefficients were obtained by deriving the unsteady TSD equation from the mass conservation equation[8].

The boundary conditions imposed on the flow field are

$\phi = 0$	far upstream	(9)
$\phi_x+\phi_t = 0$	far downstream	(10)
$\phi_z = 0$	far above & below wing	(11)
$\phi_y = 0$	far spanwise & at wing root	(12)
$\Delta\phi_z = 0$	along wake	(13)
$\Delta C_p = 0$	along wake	(14)

The condition that the flow be tangent to the wing surface is

$$\phi_z^{\pm} = f_x^{\pm} + f_t,\ 0 < x < 1,\ y < y_{tip},\ z = 0 \qquad (15)$$

where + indicates the upper surface, and - denotes the lower surface. The instantaneous wing surface position is given by f.

Finite difference solutions of (1) are obtained using an alternating direction implicit (ADI) method. The ADI method is time accurate and requires one sweep in each of the coordinate

directions to advance the solution one time increment. In XTRAN3S Version 1.5[5] Murman-Cole[3] type-dependent differencing is used for mixed flows. For reasons to be discussed later, Engquist-Osher[10] differencing is implemented for the present study.

TSD Modifications

This section describes the modifications that were made to include nonisentropic effects in TSD theory. These changes were first implemented for two-dimensional flows[4]. In the present study, they have been extended to three dimensions by applying them at each spanwise plane as though the flow in those planes was two dimensional. This technique still allows for the calculation of swept shocks. Details of the modifications are given below, although the method that is used is the same as that presented in Ref. 4.

Modified Flux

The original streamwise flux, given by (3), has been replaced by

$$f_1 = (\gamma + 1)M_\infty^2 R\,(V^* V - V^2/2) + G\phi_y^2 \qquad (16)$$

where

$$R = \frac{a^*}{U_\infty} = \sqrt{1 + \frac{2(1 - M_\infty^2)}{(\gamma + 1)M_\infty^2}} \qquad (17)$$

$$V = \frac{u}{1 + u/(1 + R)} \qquad (18)$$

$$V^* = V(u^*) = \frac{R^2 - 1}{2R} \qquad (19)$$

This new flux term is identical to that used in Ref. 4 except for the ϕ_y term which is included to model spanwise flow effects. This replacement of (3) by (16) requires only a change in the streamwise sweep of the ADI method.

Entropy Corrections

When a fluid particle passes through a shock, its entropy increases abruptly and then remains constant unless another shock is encountered. The increase in entropy results in a pressure decrease proportional to the strength of the shock. This nondimensional pressure loss, C_{ps}, is given by

$$C_{ps} = \frac{-2\Delta s/c_v}{\gamma(\gamma-1)M_\infty^2} \qquad (20)$$

where the entropy jump is found using the Rankine-Hugoniot relationship.

$$\frac{\Delta s}{c_v} = \ln\left\{T^\gamma\left[\frac{(\gamma + 1) - T(\gamma - 1)}{(\gamma + 1)T - (\gamma - 1)}\right]\right\} \qquad (21)$$

where T is the ratio of the downstream to upstream velocity normal to the shock.

For lifting cases there will be a jump in the upper and lower surface values of C_{ps}. Assuming that this jump in C_{ps}, ΔC_{ps}, is convected downstream at free stream speed, the following expression is obtained

$$\frac{\partial \Delta C_{ps}}{\partial t} + \frac{\partial \Delta C_{ps}}{\partial x} = 0 \qquad (22)$$

Equation (22) is integrated to obtain ΔC_{ps} along the wake. The condition of continuous pressure across the wake then becomes

$$\frac{\partial \Delta\phi}{\partial t} + \frac{\partial \Delta\phi}{\partial x} = \frac{1}{2}\Delta C_{ps} \qquad (23)$$

Without the nonisentropic modifications, $C_{ps} = 0$, and the usual condition

$$\frac{\partial \Delta\phi}{\partial t} + \frac{\partial \Delta\varphi}{\partial x} = 0 \qquad (24)$$

is obtained.

Finally, the entropy generated pressure is added to the linear isentropic term

$$C_p = C_{p_{Linear}} + C_{ps} \qquad (25)$$

where

$$C_{p_{Linear}} = -2(\phi_x + \phi_t) \qquad (26)$$

Engquist Osher Switching

While testing the nonisentropic modifications it was found that solutions would sometimes converge with velocity overshoots immediately upstream of shock waves. Because the resulting spike in the pressure distribution occured only at the shock, the differencing method was changed. Using Engquist-Osher differencing eliminated the velocity overshoots upstream of shocks. Although not demonstrated in three dimensions, Engquist-Osher differencing has been shown to dissipate expansion shocks and to improve code stability[5].

Results and Discussions

Flows past an infinite aspect ratio wing with a NACA 0012 section were calculated to determine if the 3-D method yields the 2-D solution for that case. For all such cases involving the NACA 0012 section the NLR coefficients were used. The effect of aspect ratio on the solution for a rectangular wing using a NACA 0012 airfoil section is presented. A wing of aspect ratio 12 was choosen for a parametric study - varying Mach number and angle of attack - to determine the effects of the nonisentropic modifications. Comparisons with solutions of the Euler equations are shown. Comparisons of steady and unsteady results for the RAE tailplane model[12] with experimental data are also shown.

NACA 0012

2-D Results

The two dimensional XTRAN3S results were obtained by calculating flow past an infinite aspect ratio rectangular wing. This study was performed in order to verify that using XTRAN3S in this manner produces the same multiple solutions as XTRAN2L.[4]

Figure 1 shows the pressure distribution on a NACA 0012 airfoil at M_∞ = 0.84 and angle of attack α = 0°. This Mach number and angle of attack were chosen because these conditions are in the middle of the 2-D nonuniqueness region for this airfoil. The three dimensional code is seen to produce the 2-D nonunique solution. The solution has converged to steady state after being perturbed by a Gaussian pulse in angle of attack. The differences in the upper and lower shock locations cause the large lift associated with this case.

The region of Mach numbers in which multiple solutions have been found to occur for the NACA 0012 airfoil is shown in Fig. 2. Two sets of results are shown, those from XTRAN2L and the 2-D results of XTRAN3S. Comparisons between these two curves show that for the NACA 0012 airfoil the nonuniqueness regions predicted by the two codes are very similar. Differences in the two results can be attributed to differences in computational grids, differencing methods, and far field boundary conditions.

Figure 3 shows lift-coefficient time histories that result from a Gaussian pulse in α of one-fourth degree at M_∞ = 0.84. The angle of attack returns to zero by 150 chords of travel. The curve calculated using the unmodified code reaches a steady state value of 0.45. Replacing the original streamwise flux, Eq. (3), with the modified flux of Eq. (16)

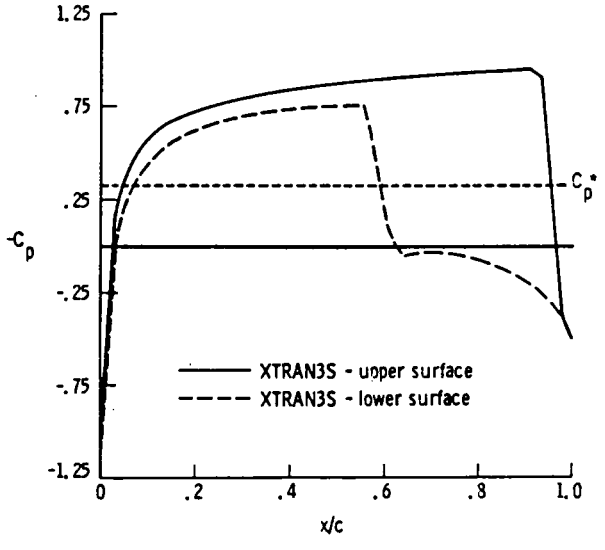

Fig. 1 Steady state pressure distribution for NACA 0012, M = .84, α = 0° using XTRAN3S simulating 2-D flow.

causes the lift to converge to a value of 0.3. When the entropy corrections, Eqs. (22) - (25), are included with the modified flux, the lift returns to zero after the pulse in angle of attack. These results are similar to those obtained by Fuglsang and Williams.[4]

3-D Results

To examine the effects of finite aspect ratio on the flow solution, calculations were made for flow conditions at which multiple solutions exist in two dimensions. For this study a rectangular, AR = 12 wing with a NACA 0012 airfoil section was used. Throughout this

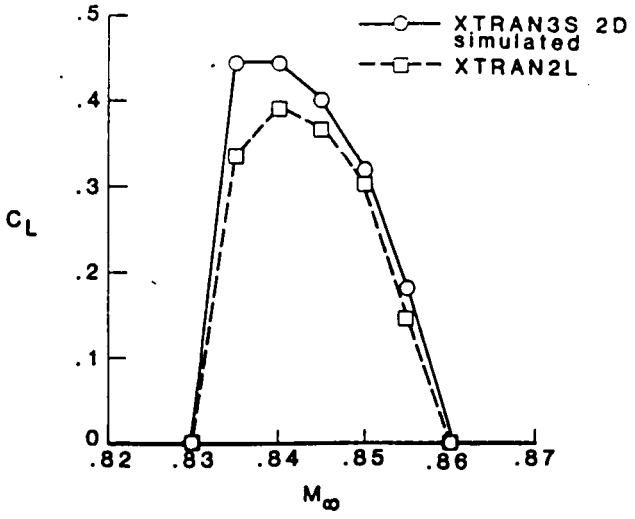

Fig. 2 Steady state 2-D lift values for the NACA 0012 at α = 0°.

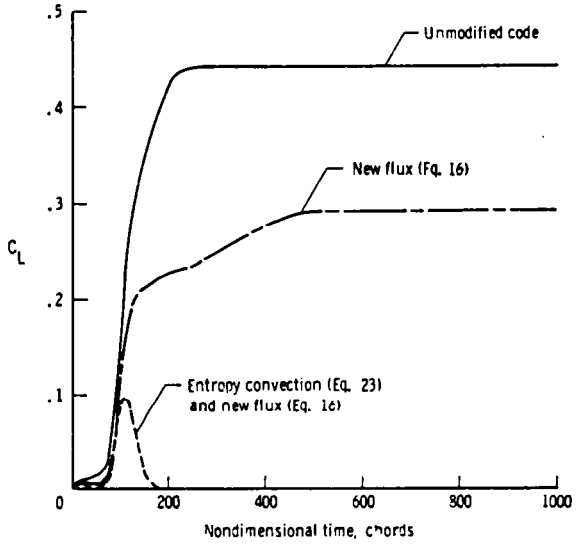

Fig. 3 Lift time histories for the NACA 0012 using a pitch pulse, amplitude = 1/4°, M = .84 with XTRAN3S simulating 2-D flow.

discussion the above wing will be referred to as "Wing A".

Figure 4 shows lift histories for various aspect ratios using the same Gaussian pulse described earlier at $M_\infty = 0.84$. These results are from the unmodified XTRAN3S code. Increasing the aspect ratio leads to nonzero lift-coefficients similar to those found in two dimensions, though at lower aspect ratios the lift returns to zero. Thus, nonunique solutions of the TSD potential equation can occur in three dimensional flow.

Figure 5 shows the steady state lift coefficient versus the inverse of the aspect ratio. The results for the rectangular wing with a NACA 0012 section at $M_\infty = 0.84$ and $\alpha = 0°$ show that multiple solutions exist for aspectratios greater than about 20 for the unmodified code. Though wings of such high aspect ratios are rare, these results demonstrate that 3-D potential flows have the same problems with multiple solutions as 2-D flows if the wing aspect ratio is large enough.

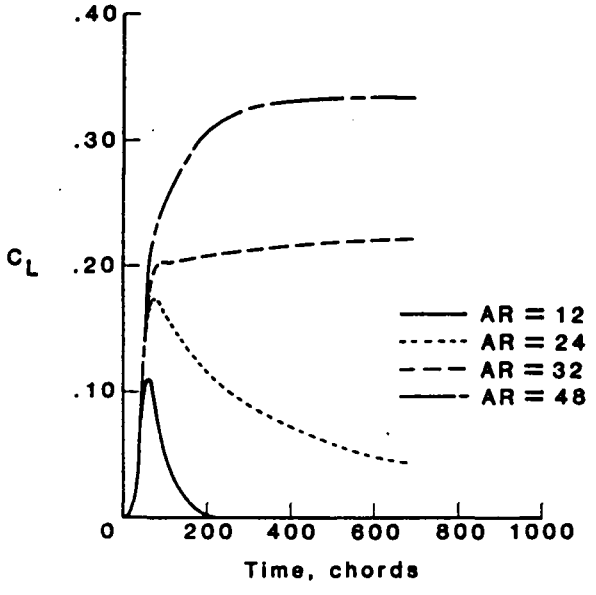

Fig. 4 Lift time histories for the NACA 0012 using a pitch pulse on various aspect ratio wings.

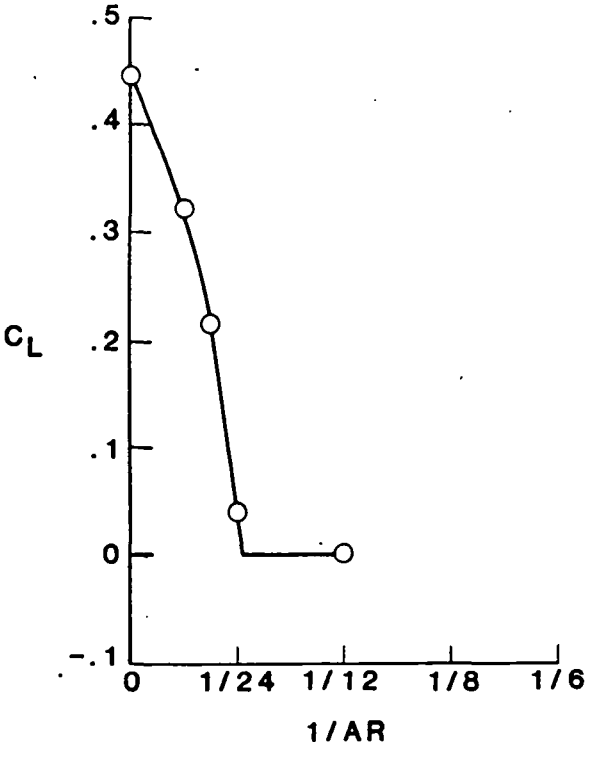

Fig. 5 Steady state lift coefficient versus aspect ratio for a rectangular wing with a NACA 0012 airfoil section at M = .84, $\alpha = 0°$.

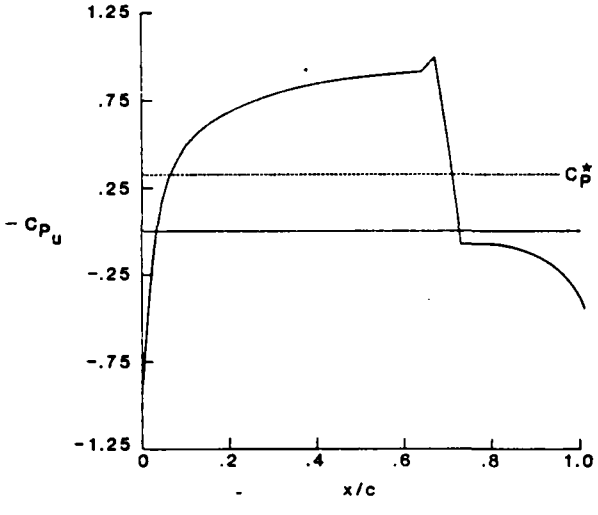

Fig. 6 Steady state pressure distribution using Murman-Cole switching.

The problem concerning the velocity overshoots when using Murman-Cole differencing is shown in Fig. 6. The cause of the overshoot is unknown although it was not encountered until the flux modifications were added to the XTRAN3S code. The overshoot occurs at various locations along the span. The use of Engquist-Osher differencing eliminated the problem as shown in Fig. 7.

Figures 8-14 illustrate the effect of the present modifications for an aspect ratio 12 wing with a NACA 0012 section at $M_\infty = 0.82$, 0.84, and 0.86. These Mach numbers were chosen because of the 2-D results shown in Fig. 2. Figures 8-10 are for M = 0.82, which is outside of the 2-D nonuniqueness region shown in Fig. 2. Figure 8 shows a comparison of steady C_L vs. α calculated using (1) unmodified XTRAN3S,

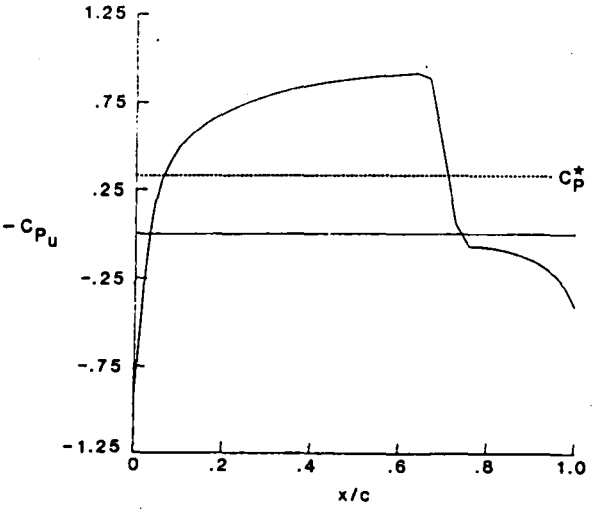

Fig. 7 Steady state pressure distribution using Engquist-Osher switching.

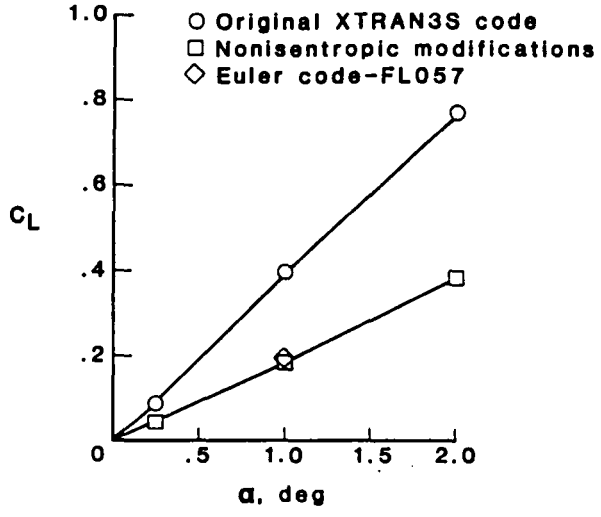

Fig. 8 Total lift coefficient versus angle of attack for wing A at M = .82.

(2) modified XTRAN3S, and (3) the FL057MG Euler code.[11] In this case, the modified XTRAN3S results agree well with the Euler calculations at $\alpha = 1°$. The lift curve slope calculated with the modified XTRAN3S code had a value approximately half that calculated using the unmodified XTRAN3S. Figure 9 shows a comparison of spanwise lift distribution at 1° angle of attack. The modified TSD theory shows excellent agreement with the Euler results except at the tip where the Euler code seems to have some difficulty, believed to be due to gridding near the tip. The corresponding comparison of the pressure distributions is shown in Fig. 10 for 1° angle of attack. Only two lower surface pressure distributions are shown since the effects of the strong shock modifications decrease toward the tip in the same manner as on the upper surface. The excellent agreement in spanwise load distribution is a result of the more accurate shock location.

Figures 11-13 show corresponding results for $M_\infty = 0.84$ which is in the middle of the nonuniqueness region shown in Fig. 2. At this higher Mach number, as shown in Fig. 11, the lift curve calculated with the original code has a very steep slope initially and then levels off (due to the shock reaching the trailing edge). The nonisentropic modifications produce a nearly linear lift curve, as does the Euler code - although the agreement with the Euler code is not as good as at $M_\infty = 0.82$.

Figures 12 and 13 show section lift distributions at $\alpha = 1°$ and 2° for $M_\infty = 0.84$. The present modifications greatly improve the agreement between TSD results and Euler results in a way similar to that shown in Fig. 9. Figure 13 also shows how the section lift from the unmodified code begins to diverge from the elliptical behavior exhibited by the Euler results. The divergence in total lift coefficient for the nonisentropic and the Euler results as the angle of attack increases is believed to be due to assumptions of TSD theory (thin wing, small angle of attack) which are less valid as the angle of attack increases.

When the Mach number is increased to 0.86 unmodified TSD theory predicts the upper surface shock location to be at the trailing edge for any significant angle of attack. Figure 14 shows that the total lift curve using the modified code is much more linear and closer to the Euler results although the lift values are high.

RAE

The nonisentropic theory was tested on the aspect ratio (AR = 2.41), tapered swept wing of the RAE tailplane model.[12] Theairfoil used is approximately the NACA 64A010.2. In order to compare with results from Ref. 13, the NASA Ames coefficients were used along with the grid transformation used by Bennett[13].

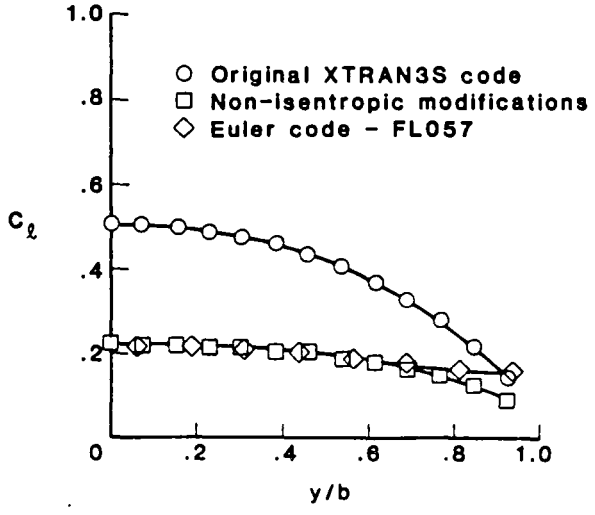

Fig. 9 Section lift coefficients versus semispan for wing A at M = .82, $\alpha = 1°$.

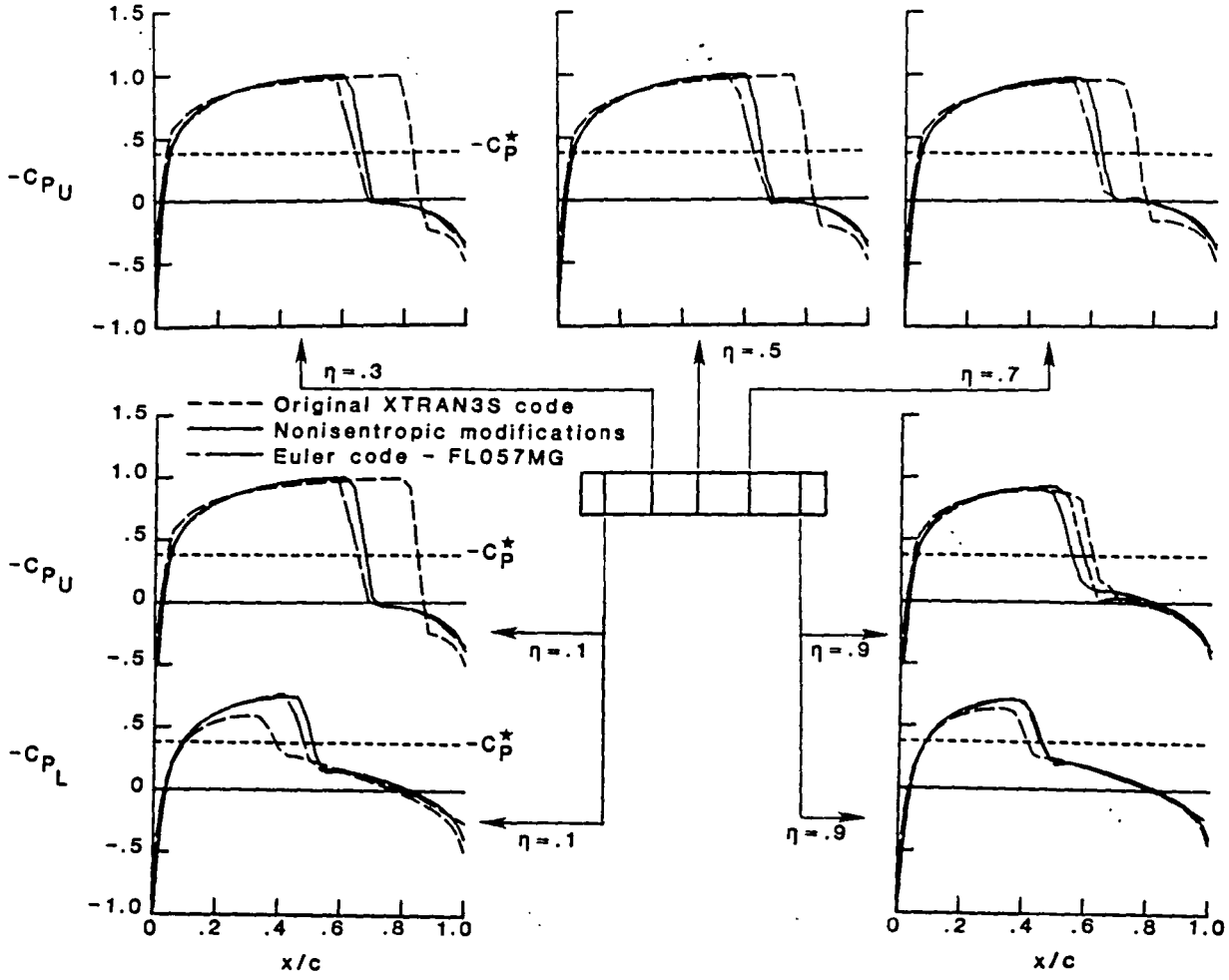

Fig. 10 Steady state pressure distribution for wing A at M = .82, α = 1°.

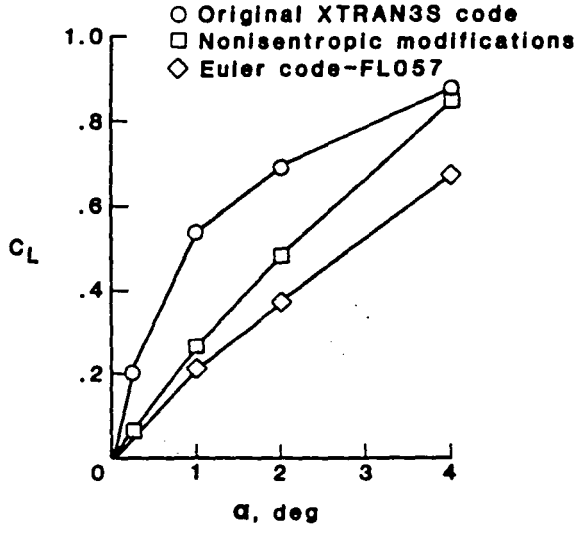

Fig. 11 Total lift coefficient versus angle of attack for wing A at M = .84.

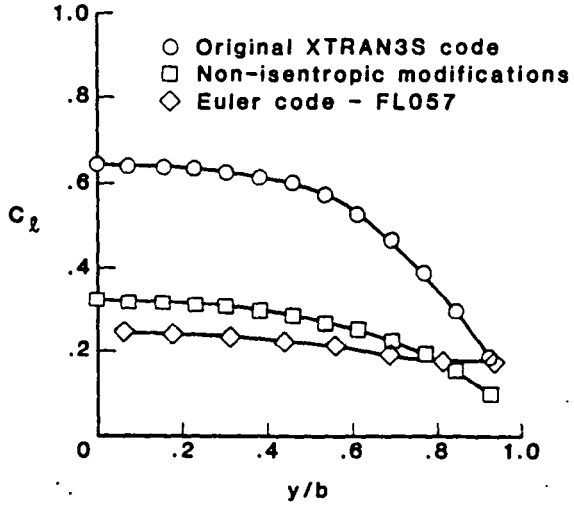

Fig. 12 Section lift coefficients versus semispan for wing A at M = .84, α = 1°.

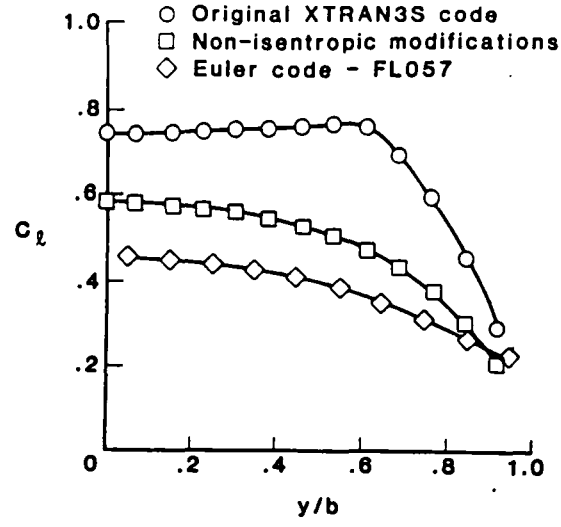

Fig. 13 Section lift coefficients versus semispan for wing A at M = .84, α = 2°.

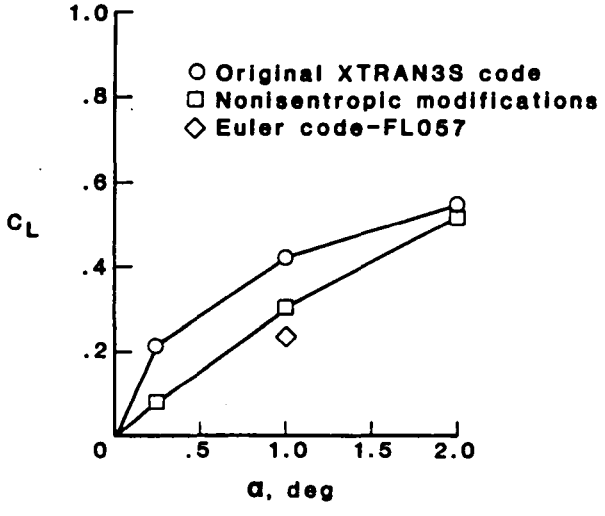

Fig. 14 Total lift coefficient versus angle of attack for wing A at M = .86.

Steady results for M = 0.90, α = -.3° with and without the nonisentropic modifications are shown in Fig. 15. As the tip of the wing is approached, the shock increases in strength and the nonisentropic modifications have their largest effect. Because the angle of attack is small for this case, the entropy convection has little effect whereas the new flux causes the largest change in the results of Fig. 15.

Unsteady results for the above case are shown in Fig. 16. For this case, the wing was oscillated at 70 Hz about α = -.3° with an amplitude of .57°. The reduced frequency used was k = .44. The center of rotation was 68 percent chord. As these results show the nonisentropic modifications result in a slight improvement in agreement with experimental data. The effects are greatest near the tip. The effects of entropy convection is greater here because the amplitude of oscillations is greater and creates a difference in shock strengths on the upper and lower surfaces.

Conclusion

Nonisentropic modifications to three dimensional transonic small disturbance (TSD) theory have been formulated. The modifications were incorporated and tested in the 3-D TSD code, XTRAN3S, for flows past a rectangular NACA 0012 wing of aspect ratio 12. A comparison of Euler solutions and the results obtained using the modified theory shows that a significant improvement was made in modeling the Euler solutions. One of the most noticeable improvements is the more accurate lift curve slope. Also discovered is the property of the unmodified code to produce multiple solutions for wings of sufficiently large aspect ratios.

The nonisentropic modifications were also tested on RAE tailplane model for steady and unsteady flows. Comparisons of modified, unmodified, and experimental results showed that the modified results improved the agreement with experiment for both steady and unsteady results particularly near the tip where the shock is the strongest.

Acknowledgements

This work constitutes a part of the first author's M.S. thesis at Purdue University and was supported by the NASA Langley Graduate Aeronautics Program under contract NAG-1-372.

References

[1]Steinhoff, J.; and Jameson, A.: "Multiple Solutions of the Transonic Potential Flow Equations." AIAA Journal, Vol. 20, No. 11, November 1982.

[2]Salas, M. D.; and Gumbert, C. R.: "Breakdown of the Conservative Potential Equation." AIAA Paper No. 85-0367.

[3]Williams, M.; Bland, S.; and Edwards, J.: "Flow Instabilities in Transonic Small Disturbance Theory." NASA Technical Memorandum 86251, January 1985.

[4]Fuglsang, D.; and Williams, M.: "Non-Isentropic Unsteady Transonic Small Disturbance Theory." AIAA Paper No. 85-0600.

[5]Whitlow, W.: "XTRAN2L: A Program for Solving the General-Frequency Unsteady Transonic Small Disturbance Equation." NASA Technical Memorandum 85723, November 1983.

[6]Borland, C. J.: "Further Development of XTRAN3S Computer Program." NASA CR 172335, May 1984.

[7]Lomax, H., Bailey, F. R., and Ballhaus, W. F.: On the Numerical Simulation of Three-Dimensional Transonic Flow with Application to the C-141 wing. NASA TN D-6933, August 1973.

[8]van der Vooren, J., Sloof, J. W., Huizing, G. H., and van Essen, A.: Remarks on the Suitability of Various Transonic Small Perturbation Equations to Describe Three-Dimensional Transonic Flow; Examples of Computa-

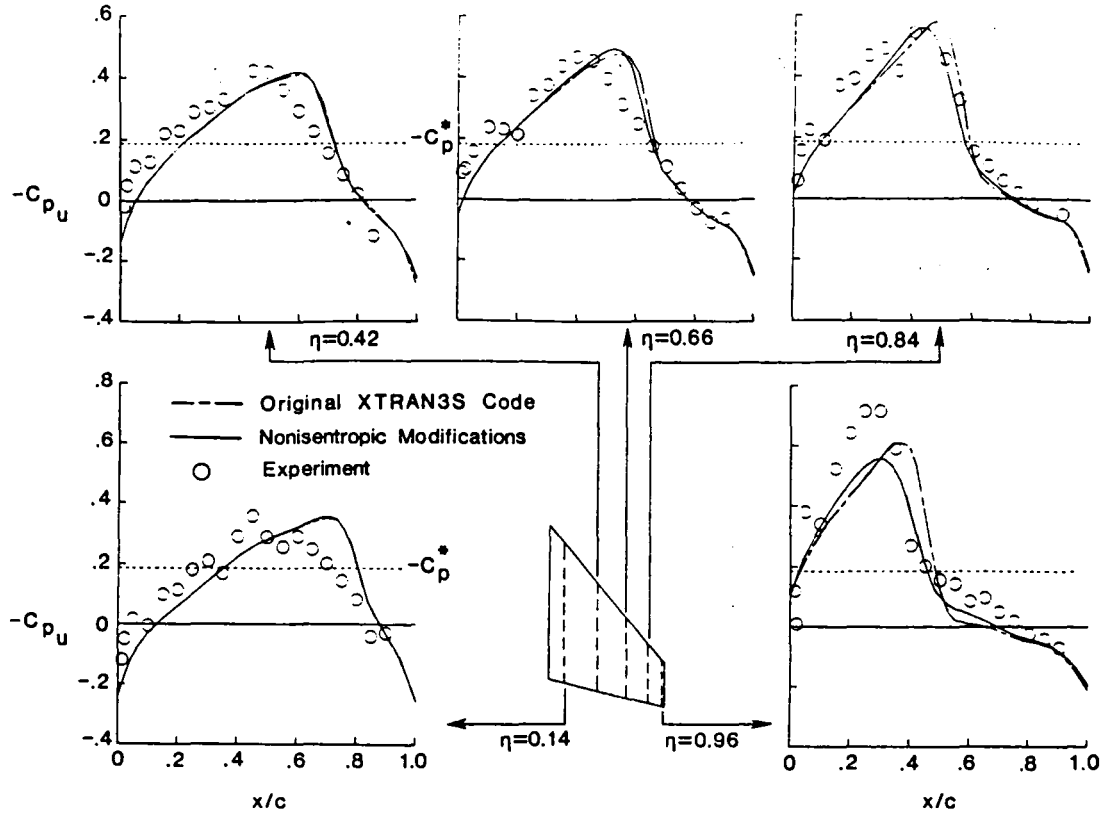

Fig. 15 Steady state pressure distribution for the RAE wing at M = 0.90, α = -.3°.

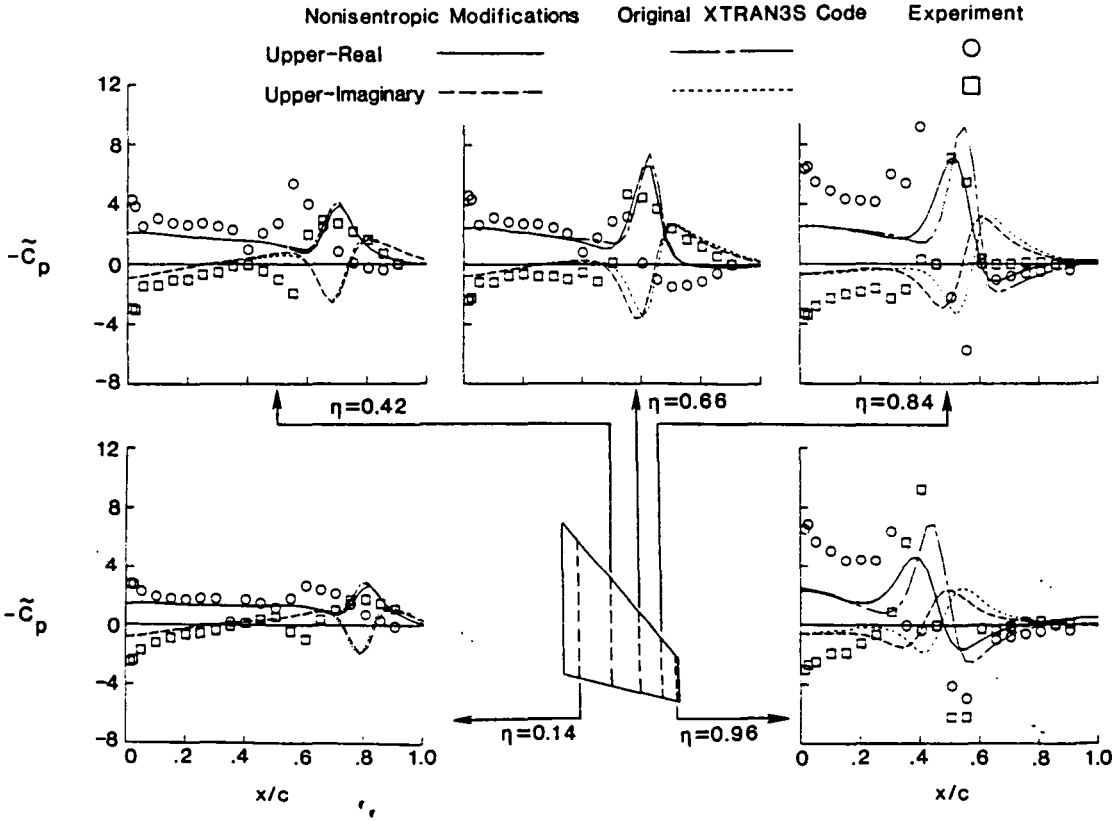

Fig. 16 Unsteady pressure distribution for the RAE wing at M = 0.90, α = -.3°.

tions Using a Fully-Conservative Rotated Difference Scheme. Symposium Transsonicum II, Gottingen, West Germany, September 1975, proceedings, Springer-Verlag, Berlin, 1976, pp. 557-566.

[9]Murman, E. M.: Analysis of Embedded Shock Waves Calculated by Relaxation Methods, Proceedings of AIAA Computational Fluid Dynamics Conference, July 1973, pp. 27-40.

[10]Engquist, B. E.; and Osher, S. J.: "Stable and Entropy Satisfying Approximations for Transonic Flow Calculations." Mathematics of Computation; Vol. 34, No. 149, January 1980, pp. 45-75.

[11]Jameson, A.; and Baker, T. J.: "Multigrid Solution of the Euler Equations for Aircraft Configurations." AIAA Paper 84-0093, 1984.

[12]Mabey, D. G., Welsh, B. L., and Cripps, B. E.: "Measurements of Steady and Oscillatory Pressures on a Low Aspect Ratio Model at Subsonic and Supersonic Speeds." British RAE Technical Report 84095, September 1984.

[13]Bennett, R. M., Wynne, E. C., Mabey, D. G.: "Calculation of Transonic Steady and Oscillatory Pressures on a Low Aspect Ratio Model and Comparison with Experiment." NASA Technical Memorandum 86449, June 1985.

1. Report No.	2. Government Accession No.	3. Recipient's Catalog No.
NASA TM-87726		

4. Title and Subtitle	5. Report Date
Nonisentropic Unsteady Three Dimensional Small Disturbance Potential Theory	April 1986
	6. Performing Organization Code 505-63-21-01

7. Author(s)	8. Performing Organization Report No.
M. D. Gibbons* W. Whitlow, Jr. M. H. Williams*	
	10. Work Unit No.

9. Performing Organization Name and Address	11. Contract or Grant No.
NASA Langley Research Center Hampton, VA 23665-5225	
	13. Type of Report and Period Covered
12. Sponsoring Agency Name and Address	Technical Memorandum
National Aeronautics and Space Administration Washington, DC 20546-0001	14. Sponsoring Agency Code

15. Supplementary Notes *Purdue University

This paper will be presented at the AIAA/ASME/ASCE/AHS 27th Structures, Structural Dynamics and Materials Conference, San Antonio, TX, May 19-21, 1986 as AIAA Paper No. 86-0863.

16. Abstract

Modifications that allow for more accurate modeling of flow fields when strong shocks are present have been made to three dimensional transonic small disturbance (TSD) potential theory. In addition, Engquist-Osher type-dependent differencing was incorporated into the solution algorithm. The modified theory was implemented and tested in the XTRAN3S computer code. Steady flows over a rectangular wing with a constant NACA 0012 airfoil section and an aspect ratio of 12 were calculated for freestream Mach numbers (M_∞) of 0.82, 0.84, and 0.86. Comparisons between results obtained using the modified and unmodified TSD theories are presented along with results from a three dimensional Euler code. Nonunique solutions in three dimensions are shown to appear for the rectangular wing as aspect ratio increases. Steady and unsteady results are shown for the RAE tailplane model at $M_\infty = 0.90$. Comparisons are made between calculations using unmodified theory, modified theory and between experimental data.

17. Key Words (Suggested by Author(s))	18. Distribution Statement
Strong Shock, Entropy, Flux, Nonisentropic, Engquist-Osher Switching, XTRAN3S	Unclassified - Unlimited Subject Category 02

19. Security Classif. (of this report)	20. Security Classif. (of this page)	21. No. of Pages	22. Price
Unclassified	Unclassified	11	A02

For sale by the National Technical Information Service, Springfield, Virginia 22161

End of Document